Synthesis and characterization of Li_2O modified sodium phosphate glasses

M. E. Sayed[a], M. M. Elokr [b], L. I. Soliman [c], H. A. Zayed [d*]

[a] Physics Department, Modern Academy for Engineering and Technology in Maadi, Cairo, Egypt
[b] Physics Department, Faculty of Science, Al-Azhar University, Cairo, Egypt
[c] National Research Center, Dokki, Cairo, Egypt
[d] Physics Department, Faculty of Women, Ain Shams University, Cairo, Egypt

Abstract

The transparent glasses 55 P_2O_5 - (45-x) Na_2O - xLi_2O where (x=0, 3, 10, 15, 30, 35) were prepared by conventional melt quenching technique. Structural and characterization have been investigated by using X-Ray diffraction (XRD) and the results show that all samples are amorphous structure. The glass transition (T_g) and crystallization temperature (T_c) are evaluated using the differential thermal analyzer (DTA), which indicate that 15 mol% Li_2O contained glasses exhibits maximum thermal stability h' of glass samples. Density, molar volume and oxygen packing density insure that Li_2O incorporated in sodium phosphate glass by increasing Li_2O content. The ac and dc electrical conductivity and dielectric constants of the prepared glass samples have been investigated. The variation of dc conductivity with the concentration of Li_2O mol% passes through a maximum at 15 mol% Li_2O. Temperature dependence of the dc conductivity of these glasses is found to obey the Arrhenius law. It reveals that the values of activation energies ΔE_{dc1} and ΔE_{dc2} at low and high temperatures lie in the range 0.452-0.93 eV. Also it was found that the values of σ_{dc} to be the same as the values obtained from the impedance study. Conductivity mechanism for grain resistance at room temperature was discussed using Cole-Cole plot. To determine the conduction mechanism, the ac conductivity and its frequency exponent have been analyzed by correlated barrier hoping model (CBH). It was found that the exponent (s) has values between 0.62-0.9; consequently the (CBH) seems to be the most interesting model related to the obtained results. The variation of dielectric constants ε' and ε'' with the concentration of Li_2O mol% pass through a maximum at 15 mol% Li_2O and this result would be discussed by means of dielectric polarization mechanism of material. The maximum value of the maximum barrier height W_m obtained from Guitini equation was found to increase with increasing of Li_2O mol%.

Keywords: Sodium Phosphate glass; Thermal analysis; Electrical conductivity.

***Corresponding Author:** dr.mohamed_essam@yahoo.com

1- Introduction

The synthesis and physical properties of phosphate glasses have attracted much attention because of their potential application in technology. Phosphate glasses possess a series of interesting and unique physical properties better than other glasses such as hardness, transparency at room temperature, sufficient strength, low glass transition temperature, excellent corrosion resistance, high electrical conductivity, low melting and softening temperature and high thermal expansion [Yahia H. Elbashar et al. (2016), R. K. Brow (2000), Samir Y. Marzouk (2009), A. Bhide et al. (2007), R. K. Brow (2000), I. Abrahams et al. (2000)]. Among oxide glasses, sodium and lithium phosphate glasses / glass-ceramics are used as solid electrolytes for battery applications [Paramjyot Komarjha et al. (2015), A. Yamano et al. (2014)]. Phosphate glasses have been considered as a promising group of glasses for optical amplifiers, fibers, etc. [A V. Chandrasekhar et al. (2003), Nehal Aboulfotoh et al. (2014)] and also play various important roles in laser systems. For laser application glasses used as transmitting optical components, as modulators, for photonic switching and magneto-optic materials [D. D. Ramteke et al. (2017)]. By varying the glass composition, glasses with specific properties can be achieved. Dc electrical properties of lithium metal oxide containing phosphate glasses like Li_2O – CdO – P_2O, Li_2O – MnO – BeO_3 ….. etc, have been studied with the change of concentration of the modifier or glass former [M. Altaf et al. (2001), Peipei Chen et al. (2015), V. C. Veerana et al. (2005)]. Sodium phosphate glasses are in a great demand because of their strong glass forming nature, low crystallization and melting temperature. It is expected that the replacement of Na_2O by Li_2O in P_2O_5 based glasses exhibit better ionic conductivity due to smaller size of Li^+ ($0.76A^o$) as compared to Na^+ ($1.02A^o$). The conductivity is generally studied as a function of temperature, and it may also depend on structural changes in the glasses. Recently the structural and thermal properties of P_2O_5 – Na_2O – Li_2O and Li_2O – Na_2O – P_2O doped with La_2O_3 has been reported in literature [Paramjyot Komarjha et al. (2015), A. Yamana et al. (2014), Peipei Chen et al. (2015)]. It was found that the structural properties of P_2O_5 – Na_2O – Li_2O glasses strongly depend on Na_2O and Li_2O content.

In the literature, we find that the dc and ac electrical conductivity of P_2O_5 – Na_2O – Li_2O glasses have not been studied extensively for this reason, the present work gives the preparation method and deals with the dc and ac electrical conductivity and structure properties of P_2O_5 – Na_2O – Li_2O glasses over a wide range of composition, temperature and frequency to determine the possible conduction mechanisms and to determine the activation energy and also to propose the crystallization mechanism of the prepared glasses.

2- Experimental

The transparent 55 P_2O_5 – (45-x) Na_2O – x Li_2O, (x = 0, 3, 10, 15, 30, 35) glasses used in the present study were prepared from high purity analytical grade chemicals $(NH_4)_2HPO_4$, Na_2CO_3 and LiCl by conventional melt quenching technique. The appropriate quantities of these chemicals were weighed and mixed in agate mortar and were hand ground for about one hour. The batches were initially kept at 400 C^o in porcelain crucibles to release volatile products coming from the starting materials and then melted in an electric furnace with intermediate stirring at 1000 C^o for one hour to ensure homogeneity of the glasses. Samples of the desired shape were obtained by quenching the melt at 350 C^o between two preheated stainless steel plates for two hours to eliminate the mechanical and thermal stresses produced during casting and collected the next day. The prepared glass samples were polished by silicon carbide water proof abrasive papers of various grades ranging between 320 and 1000 to achieve a good optical transparency samples.

Glass transition temperature (T_g) and crystallization temperature (T_c) were determined using deferential thermal analysis (DTA) at heating rate 10 K^o/min.

Density measurements of the prepared samples were determined at room temperature using Archimedes principle. The mass of the glass samples were measured with a Precisa 205A balance sensitive to 0.1 mg. Toluene (ρ_T =0.85455 gm/cm^3) was used as an immersion liquid.

The equation used for density calculation is given by

$$\rho_{sample} = [W_a / (W_a - W_T)]\ \rho_T \qquad (1)$$

Where ρ_{sample} is the density of the sample, W_a is the weight of sample in air, W_T is the weight of sample in toluene and ρ_T is the density of toluene. The relative error in these measurements was about 1 mg/cm^3.

The amorphous nature of synthesized glass samples was confirmed by (PANalytical PRO X'Pert Data) diffractometer which was operated at 40 KV and 45 mA and using CuKα radiation source of wavelength 1.5406 A^o with Ni filter at room temperature.

X-Ray diffraction patterns were recorded in 2Ɵ range between 4 and 90 degree with scanning rate 2 degree/min.

For dc and ac electrical conductivity a glass samples, coated with silver paint on both sides were used for the measurements and using a special designed holder.

The dc and ac electrical resistance R for the prepared samples was carried out in the temperature range (300-512K). The sample temperature was measured and controlled by using a calibrated Chromel-Alumel thermocouple connected to (TCN4M-24R Aulonics-Korea) temperature controller. For AC electrical conductivity measurements a programmable automatic LCR bridge (Hioki, 3532-50) was used in a wide frequency range (50 Hz to 5 MHz).

3- Results and discussion

3.1 X-Ray Diffraction (XRD)

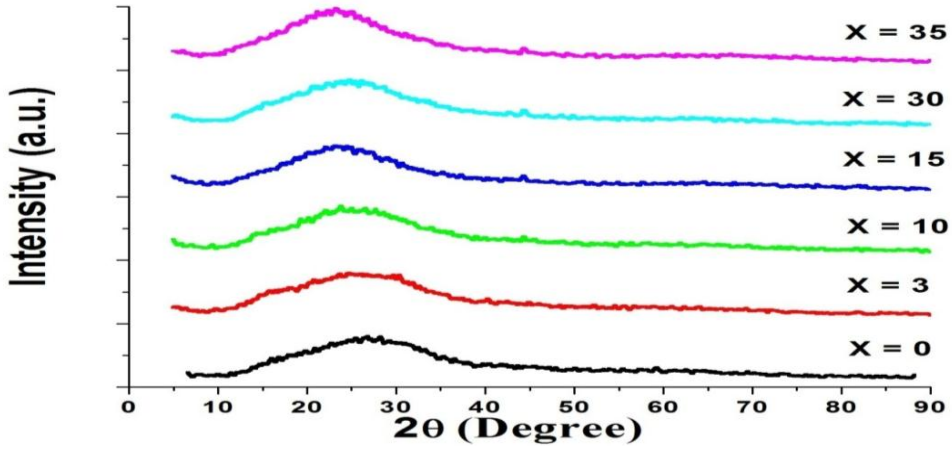

Fig.1. XRD diffraction patterns of 55 P_2O_5 – (45-x) Na_2O – x Li_2O glass samples at different composition of Li_2O (mol.%).

Fig.1 shows XRD patterns of the prepared glass samples 55 P_2O_5 – (45-x) Na_2O – x Li_2O (x= 0 – 35 mol% Li_2O) at room temperature. The presence of one broad hump in the range of 15 – 35 for all the investigated samples indicated their amorphous nature and the absence of phase separation.

3-2 Differential thermal analysis (DTA)

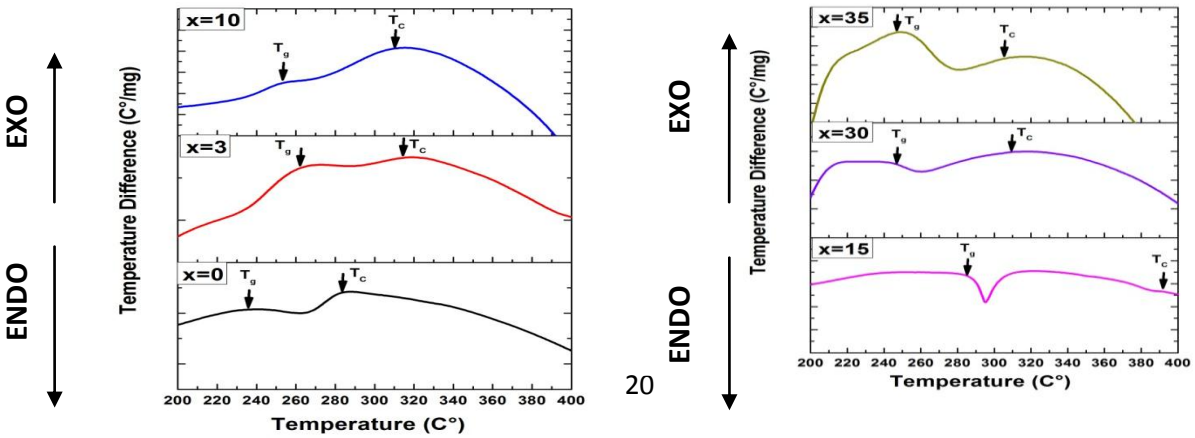

Fig.2. DTA patterns of 55 P_2O_5 – (45-x) Na_2O – x Li_2O glass samples at different composition of Li_2O (mol.%).

Fig.2 shows the DTA patterns of 55 P_2O_5 – (45-x) Na_2O – x Li_2O glass samples (x= 0, 3, 10, 15, 30, 35). The DTA patterns are used to determine the glass transition temperature T_g , the crystallization temperature T_c and the glass thermal stability $h' = (T_c - T_g) / T_g$. The determined data is given in Table 1.

Table 1: Glass transition temperature (T_g), crystallization Temperature (T_c) and glass stability (h') of different glass compositions.

Composition of 55 P_2O_5 – (45-x) Na_2O – x Li_2O x (mol %)	T_g (c^o)	T_c (c^o)	ΔT (c^o)	$h' = \Delta T/T_g$
0	234.42	283.56	49.14	0.20962
3	262.13	317.79	55.66	0.21234
10	252.65	310.28	57.63	0.2281
15	285.88	391.05	105.17	0.36788
30	247.52	308.69	61.17	0.24713
35	243.69	305.59	61.9	0.25401

The value of h' is indicative of the thermal stability of the glass samples [Yang Lia et al. (2017)]. From Table 1 it is observed that as the concentration of Li_2O increases from 3 to 10 mol % Li_2O and from 15 to 35 mol % Li_2O T_g and T_c are found to decrease. In this case Li_2O is acting as a strong network modifier, which creates non-bridging oxygen. The non-bridging disrupt the long chains and break the chemical bonds causing a decrease in T_g and T_c. It is also observed that with increasing the concentration of Li_2O from 10 to 15 mol % T_g and T_c increases, this can be explained on the basis of nature of bonding present in the glass system [Paramjyot Komarjha et al. (2015)]. Lithium has electronegativity (0.98) which is higher than sodium (0.93). As a result P-O-Li and Li-O bonds, formed within the glass system might exhibit higher covalent character than P-O-Na and Na-O Bonds [S. Rani et al. (2008)]. The value of glass thermal stability h' for the glass sample with Li_2O content 15% mol% is found to be maximum, which indicates its highest thermal stability than other glasses.

3-3 Density, molar volume and oxygen packing densities

Transparent and bubble free glasses were obtained for the compositional series of 55 P_2O_5 – (45-x) Na_2O – x Li_2O (x=0 – 35 mol% Li_2O). The values of the experimental density (ρ_{exp}) and the theoretical density (ρ_{th}) molar volume (V_m) and oxygen packing density (OPD) are listed in Table 2 and graphically presented in Fig.3 and Fig.4.

Table 2: Experimental (ρ_{exp}) and theoretical (ρ_{the}) density, molar volume (V_m) and oxygen packing density (OPD) of different glass compositions.

Composition of 55 P_2O_5 – (45-x) Na_2O – x Li_2O x (mol %)	ρ_{exp} (gm/cm^3)	ρ_{the} (gm/cm^3)	V_m (cm^3/mol)	OPD (mol/litre)
0	2.962	2.81	36.224	88.3391
3	2.668	2.57	39.821	80.3559
10	2.419	2.3	42.911	74.5735
15	2.37	2.27	43.061	74.3139
30	2.364	2.268	40.171	79.66
35	2.361	2.267	39.397	81.2253

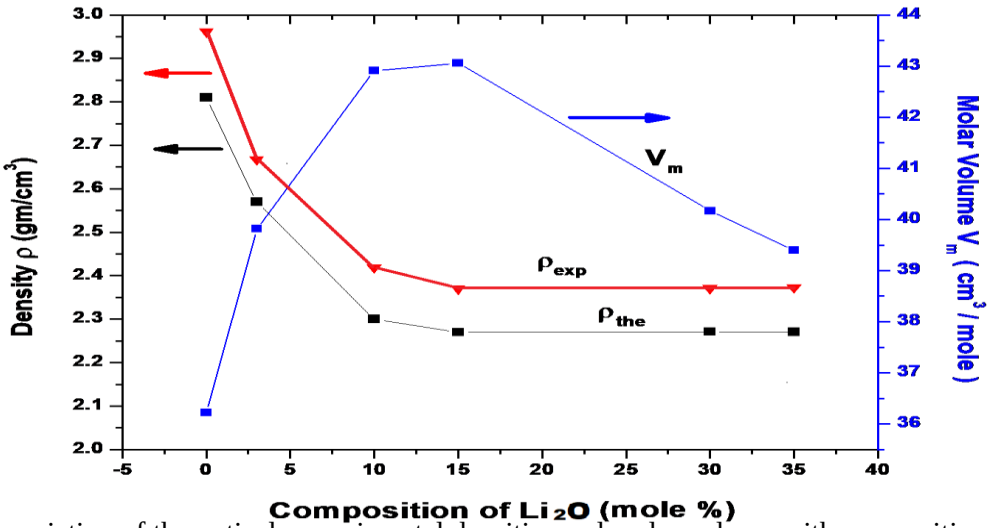

Fig.3. The variation of theoretical, experimental densities and molar volume with composition of Li_2O (mol %).

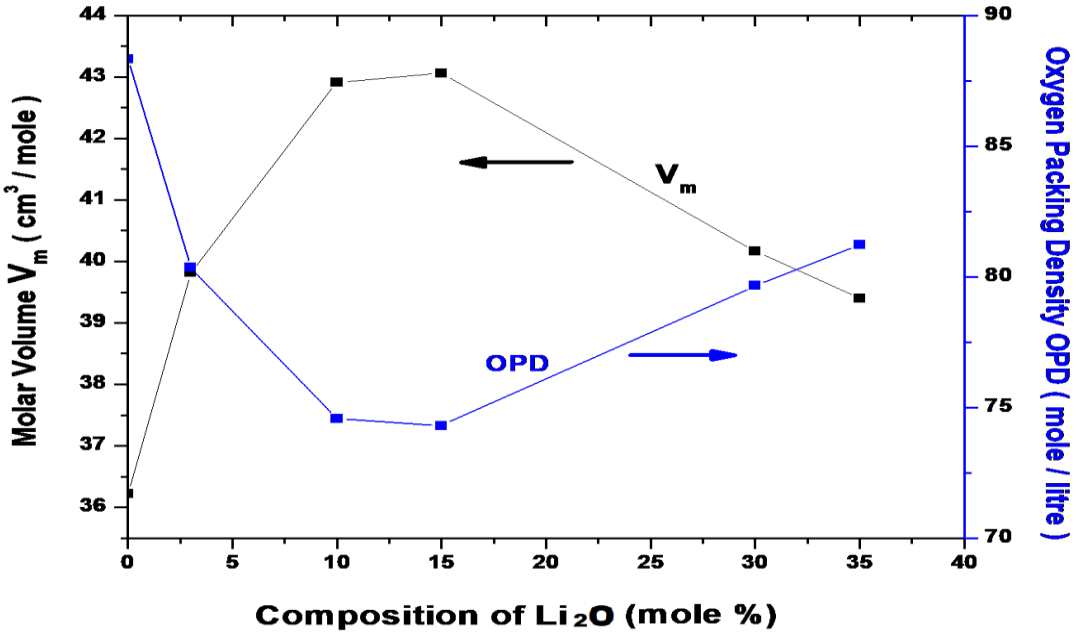

Fig.4. The variation of oxygen packing density and molar volume with composition of Li_2O (mol %).

It is found from Fig.3 that the theoretical and experimental values of density decrease with increasing concentration of Li_2O and the molar volume pass through maximum at 15 mol% Li_2O. The density decreases because the molar mass of Li_2O (29.28 g/mol) is lower than that of molecular mass of Na_2O (61.97 g/mol). The experimental density values decreases from 2.962 g/cm^3 to 2.361 g/cm^3 for the prepared glass with increasing x from zero to 35 which are in well agreement with reported values [L. Bih et al. (2008)]. This could be also explained by considering the fact that a high density Na_2O (2.2 gm/cm^3) is replaced by low density Li_2O (2.01 g/cm^3) which caused the decrease in mass density of the glass. Lithium oxide is a known glass modifier. The addition of glass modifier (Li_2O) do not contribute in glass formation but cleaves the structure of glass network and causes an increase in the molar volume of the glass [Kirk Othmar (1963)].

Oxygen packing density which is a measure of the tightness of packing of the oxide network can be used to explain the decreasing of T_g with the increase of Li_2O content. It can be seen from Fig.4 that OPD decreases from 88.3 to 74.3 mole/liter as the concentration of Li_2O increases from zero to 15 mol%. This indicates that the structure becomes loosely packed with increase in the concentration of Li_2O and the formation of a more open macromolecular chain in the prepared glass samples leading to decrease in T_g. By increasing the concentration of Li_2O from 15 to 35 mol% it was found that the

oxygen packing density increases from 74.3 to 81.2 mole/liter as the concentration of Li_2O increases from 15 to 35 mol%.

3-4 Electrical conductivity

3-4-1 dc electrical conductivity

Fig.5 shows the temperature dependence of dc electrical conductivity of 55 P_2O_5 – (45-x) Na_2O – x Li_2O ($0 \leq x \leq 35$) at different concentrations of Li_2O (mol%). The electrical conductivity σ_{dc} is thermally activated process and important to describe electrical behavior of a material. The data fit the Arhenius equation $\sigma_{dc} = \sigma_o \exp(-E_a / kT)$, σ_o is the pre-exponential factor which including the charge carrier mobility and density of states, E_a is the thermal activation energy for conduction and k is the Boltzmann constant.

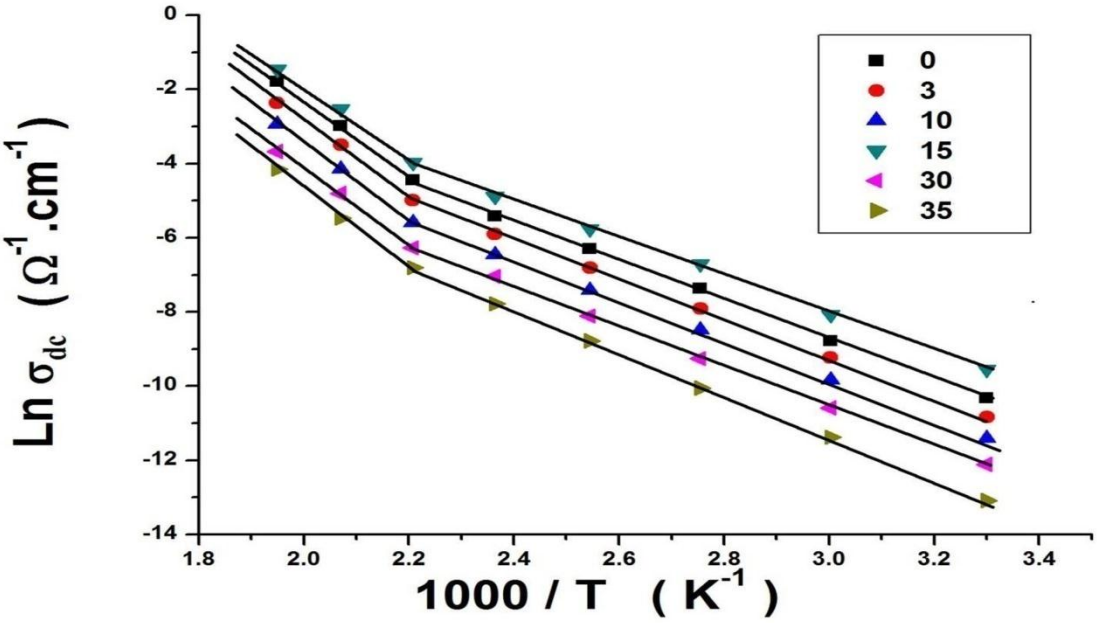

Fig.5. The variation of Ln σ_{dc} versus 1000/T for 55 P_2O_5 – (45-x) Na_2O – x Li_2O glass samples at different composition of Li_2O (mol.%).

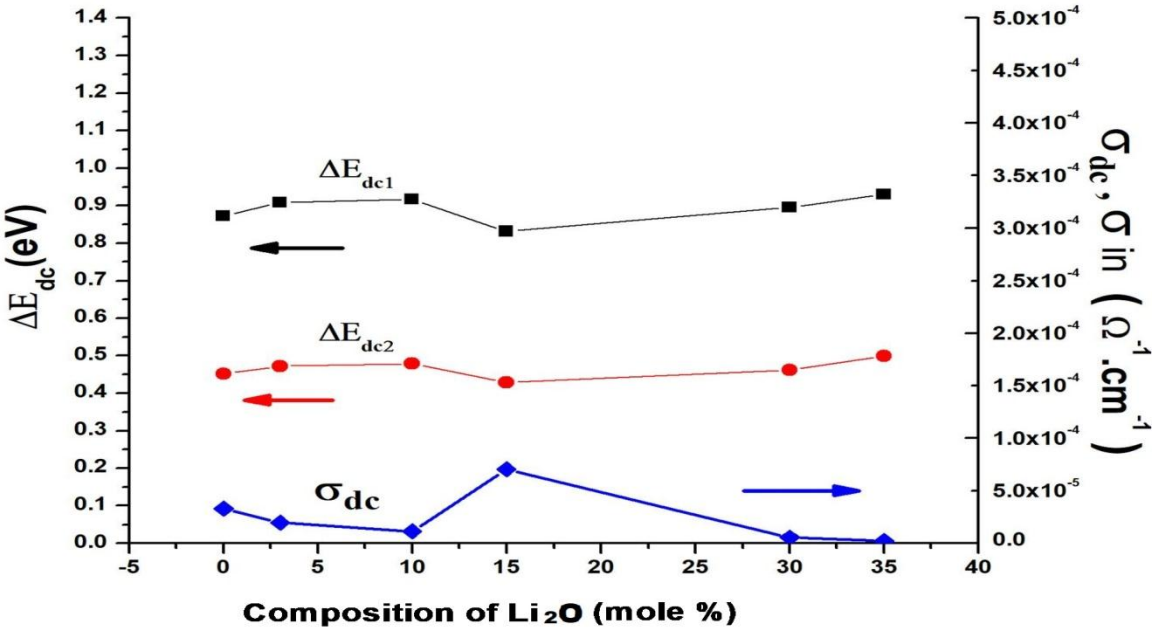

Fig.6. The variation of activation energies ΔE_{dc1} and ΔE_{dc2} and σ_{dc} at room temperature with the composition of Li_2O (mol%).

As shown in Fig.5 there are two linear regions of conductivity that gave two activation energies ΔE_{dc1} and ΔE_{dc2} which indicating the conduction mechanism in the investigated temperature range (303K – 413K). The activation energies ΔE_{dc1} and ΔE_{dc2} arise from impurity scattering. Fig.6 represents the variation of σ_{dc} at room temperature and the activation energies ΔE_{dc1} and ΔE_{dc2} with the concentration of Li_2O (mol%). It is clear from Fig.6 that σ_{dc} decreases from $3.3x10^{-5}$ to $1x10^{-5}$ $(\Omega.cm)^{-1}$ with increasing of Li_2O concentration from zero to 35 mol% Li_2O and the plot is found to exhibit a maximum for x = 15 mol% of Li_2O. In order to explain this behavior one must note that these ternary glasses were fabricated by adding different amount of Li_2O to binary sodium-phosphate glass. The sodium ions were gradually replaced by lithium ions because the amount of glass former P_2O_5 was fixed at 55 mol%. Further addition of Li_2O concentration from 10 to 15 mol% leads to increase in σ_{dc} up to $7x10^{-5}$ $(\Omega.cm)^{-1}$. Such behavior is likely to arise due to the structural changes accusing in phosphate network then decrease again up to $2.1x10^{-6}$ $(\Omega.cm)^{-1}$ at Li_2O concentration 35 mol%. The activation energies calculated from analysis of Ln σ_{dc} versus 1000 / T plots is found to increase with increasing Li_2O content to 10 mol% and then decrease with increasing Li_2O content to 15 mol% and increase again.

3-4-2 ac electrical conductivity

The measured total conductivity σ_t , can be considered a summation of σ_{dc}, and ac conductivity, σ_{ac} .At very low frequency region σ_{dc} is independent of frequency and appears as a flat dc plateau in this region of frequency. The ac conductivity is approximately independent of the frequency at lower frequencies, but more frequency dependent in high frequency region. The total conductivity follows the relation:

$$\sigma_t = \sigma_{dc}\,(\omega=0) + \sigma_{ac}\,(\omega) \qquad (2)$$

In this relation, the dc conductivity is taken to represent the ac conductivity at ω tends to zero. The ac conductivity has been analyzed used Almond-West type power law with single exponent [D. P. Almond et al. (1984)].

$$\sigma_{ac} = A \,.\, \omega^{s} \qquad (3)$$

Where A is a temperature dependent constant, $\omega = 2\pi f$ is the angular frequency and s is the frequency exponent which depend on temperature. Such a dependence on temperature determines the ac conduction mechanism and has been found to be material dependant.

3-4-2-1 Complex impedance analysis

Complex impedance is a powerful technique for the characterization of electrical properties of polycrystalline sample such as conductivity, dielectric behavior ….. etc. It may be used to explain the dynamics of mobile or bound charges in the grain or grain boundaries. The expression of real (Z') and imaginary (Z") components of the impedance (Z) can be expressed by the following relationships:

$$Z = Z' - jZ'' \qquad (4)$$

$$Z' = Z \cos Q \qquad (5)$$

$$Z'' = Z \sin Q \qquad (6)$$

Where $Q = 1 / [\, C \,.\, Z \,.\, (2\Pi f)\,]$

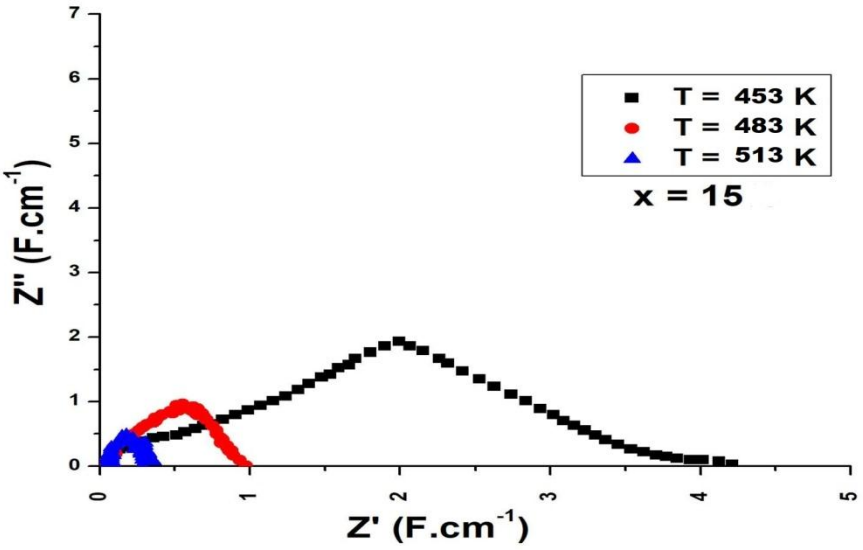

Fig.7 (a). Cole-Cole plots of Z' and Z" at 3 MHz of 55 P_2O_5 – (45-x) Na_2O – x Li_2O glasses containing 15 mol% Li_2O at different temperatures

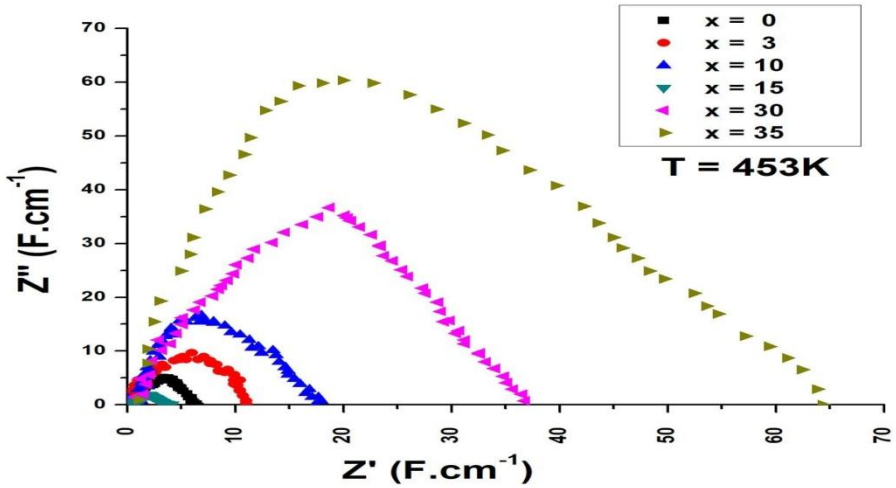

Fig.7 (b). Cole-Cole plots at 3 MHz and 453 K for different concentrations of Li_2O mol%

Fig.7-a shows the plot of Z' versus Z" (Cole-Cole plot) at 3 MHz for glass sample (with x = 15 mol% Li_2O) at different temperature, Fig.7-b Cole-Cole plots of Z' and Z" for glass samples with different compositions of Li_2O mol%. The impedance plots of all the samples were found to exhibit good single semicircle starting from the origin over the entire range of temperature and the composition studied. The absence of

second semicircle in the complex impedance plots indicates that the glass samples have only grain effect to the conductivity mechanism at room temperature.

The values of dc conductivity were calculated by taking the intersection points of semicircles on the Z' axis [M. J. Miah et al. (2016)]. From Fig.7-a it was found that the diameter of the semicircle decreasing and the intersection points of the semicircles shifted to lower Z' values with increasing temperature which suggests that the value of grain resistance is decreasing and σ_{dc} increasing with increasing temperatures. It is obvious from Fig.7-b that the diameter of the semicircle decreasing and the intersection points of semicircles shifted to lower Z' values with decreasing Li_2O content in glass samples and the value of grain resistance is decreasing to minimum. For glass sample 15 mol% of Li_2O content it was found that it has the smallest diameter of semicircles which indicating the least value of grain resistance.

To compare the obtained data of σ_{dc} calculated from Cole-Cole and σ_{dc} calculated from σ_t versus frequency are listed in Table 3. It is clear from the Table 3 that σ_{dc} (Cole-Cole) and σ_{dc} (σ_t Vs f) approximately have same values.

Table 3: values of σ_{dc} (Cole-Cole) and σ_{dc} (σ_t Vs f) at different temperatures

T(k)	σ_{dc} (Cole-Cole)	σ_{dc} (σ_t Vs f)
453	0.0188	0.0186
483	0.084	0.089
513	0.214	0.23

3-4-2-2 Frequency and temperature dependence of ac electrical conductivity

Fig.8 shows the frequency dependence of ac electrical conductivity at different temperatures for 55 P_2O_5 – (45-x) Na_2O – x Li_2O (with x = 15 mol% Li_2O). The ac conductivity behavior of all the other glass samples (with x = 3, 10, 30, 35 mol% Li_2O) is qualitatively similar. It is shown from Fig.8 that the ac conductivities exhibit a change of slope to higher values as the frequency is increased.

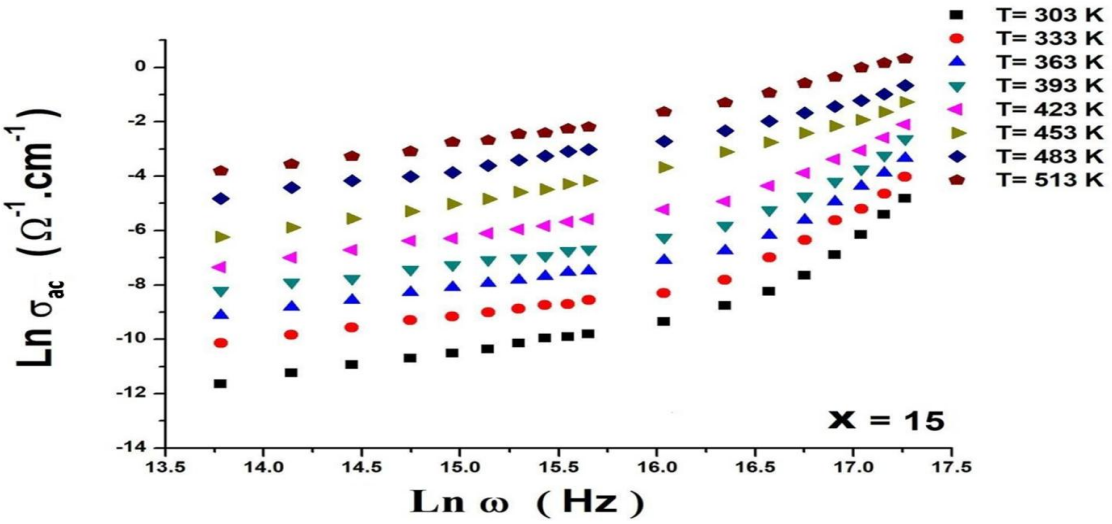

Fig.8. Frequency dependence of σ_{dc} for 55 P_2O_5 – (45-x) Na_2O – x Li_2O glasses containing 15 mol% Li_2O at different temperatures

The increase of σ_{ac} with increasing frequency suggests that hoping conduction prevails and the increase of the applied frequency enhances the hopping of charge carriers between the localized states [A. Ben Rasem et al. (2009)].

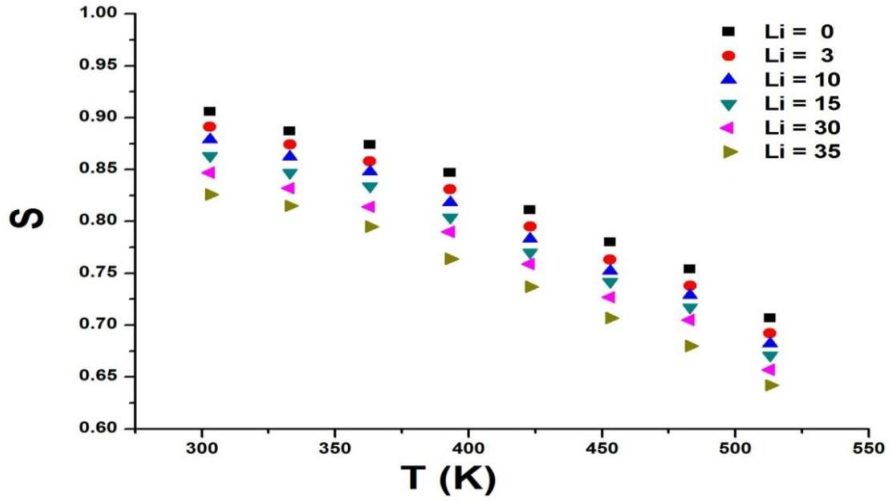

Fig.9. Temperature dependence of the frequency exponent S at different concentrations of Li_2O mol%

Values of the exponent s were calculated from the slopes of these lines at different temperatures. The temperature dependence of s for all the prepared glass samples with different concentrations is shown in Fig.9 in which s decreases with increasing temperature and the concentration of the modifier oxide (Li_2O). Also it was found that for all the prepared glass samples s values are significantly lower than unity and lie between 0.62-0.9.

According the correlated barrier hopping (CBH) model values of s decrease with increasing temperatures, this is in good agreement with the obtained results, as shown in Fig.9. Accordingly the frequency dependence of σ_{ac} can be explained in terms of CBH model. This model first developed by Pike [G. E. Pike (1972)] for single electron hoping and has been extended by Elliot and Chen [S. R. Elliot (1978), R. H. Chen et al. (2006)] for simultaneous two electron hoping

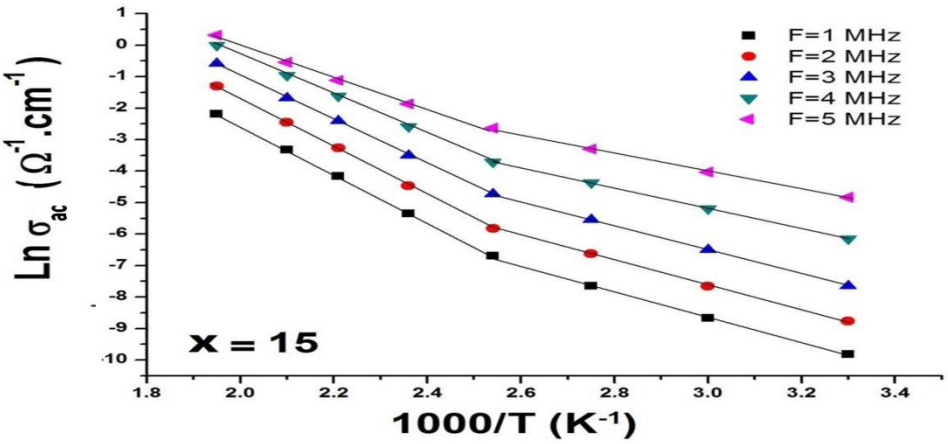

Fig.10. Temperature dependence of ac conductivity for glasses containing 15 mol% Li_2O at different frequencies

Fig.10 shows the variation of Ln σ_{ac} with the reciprocal of temperature 1000 / T in the investigated temperature range at different frequencies for 55 P_2O_5 – 30 Na_2O –15 Li_2O glass sample. This dependence of ac conductivity on temperature suggests that the ac conductivity is a thermally activated process. The value of the activation energies ΔE_{ac1} and ΔE_{ac2} has been calculated from the slope of Ln σ_{ac} versus 1000 / T curves.

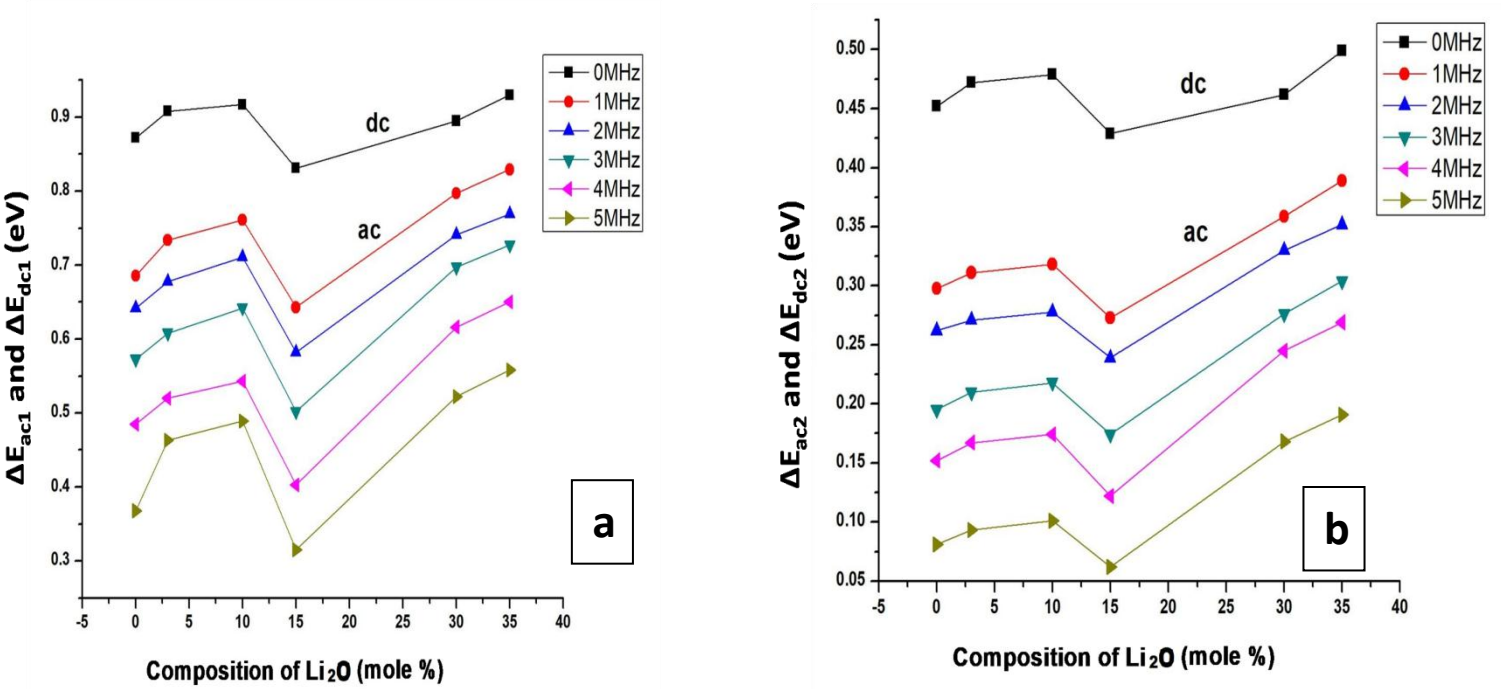

Fig.11 (a). The variation of ac activation energies (a) ΔE_{ac1} and (b) ΔE_{ac2} with the concentration of Li_2O mol% at different frequencies

Fig.11 (a,b) shows the variation of the activation energies ΔE_{ac1} and ΔE_{ac2} with concentration of Li_2O mol% at different frequencie. It is found that the activation energies ΔE_{ac1} and ΔE_{ac2} increase with increase of Li_2O concentration and the plot is found to exhibit minimum at X = 15 mol% Li_2O, also it is observed that the behavior of both ΔE_{dc} and ΔE_{ac} are almost the same, Such increase can be attributed to the contribution of the applied frequency to the conduction mechanism, which confirms the hopping conduction to be dominant mechanism [Sh. A. Mansour et al. (2010)].

3-4-2-3 Temperature and frequency dependence of dielectric constant ε' and ε"

The complex dielectric constant of the investigated samples is formulated with two parts, $\varepsilon = \varepsilon' + i\,\varepsilon''$; where ε' is the real part of dielectric constant and it is a measure of the energy, stored from the applied electric field in the material and identified the strength of alignment of dipoles in the dielectric. ε" is the imaginary part of dielectric constant and it is the energy dissipated in the dielectric. ε' and ε" were evaluated using the following relations:

$$\varepsilon' = C\,L / \varepsilon_o\,A \qquad (7)$$

$$\varepsilon'' = \varepsilon' \tan\delta \qquad (8)$$

Where C is the capacitance of the sample, ε_o is the free space permittivity, L is the sample thickness and A is the area and tan δ is the dissipation factor.

The real and imaginary parts of dielectric constant ε' and ε'' of 55 P_2O_5 – 30 Na_2O –15 Li_2O glass samples with different concentration of Li_2O are measured over frequency range from 50 Hz to 5 MHz.

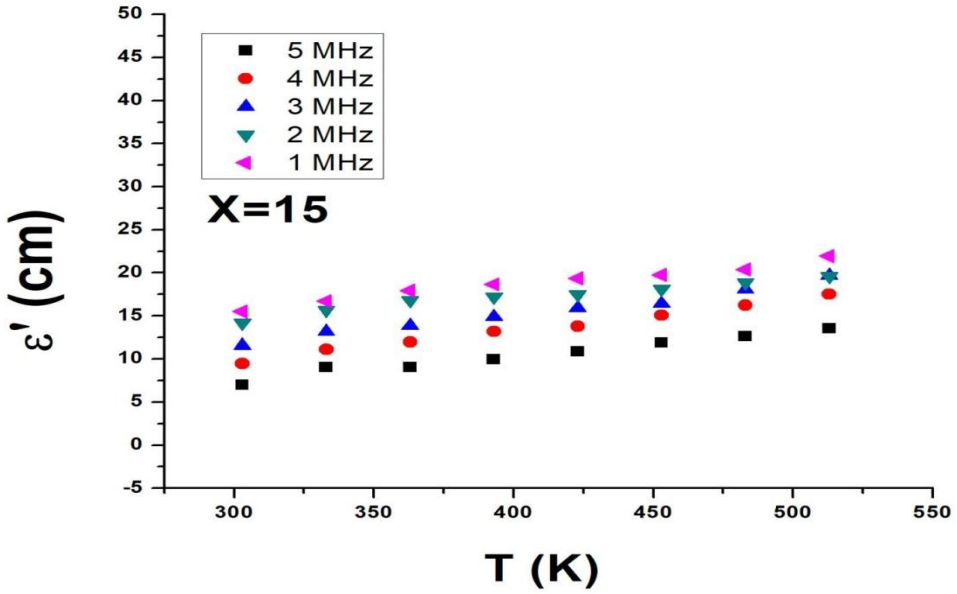

Fig.12. The temperature dependence of real part (ε') of glass containing 15 mol% Li_2O at different frequencies

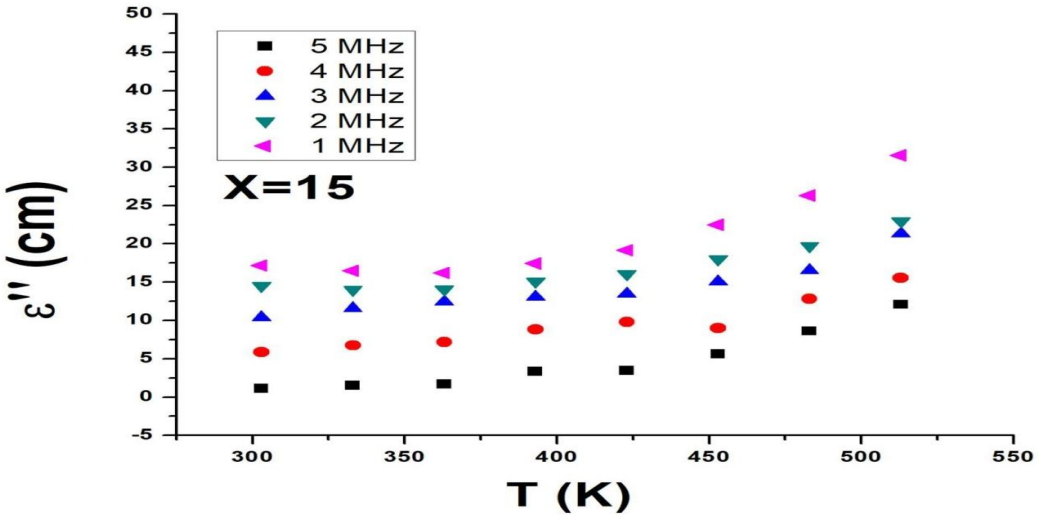

Fig.13. The temperature dependence of imaginary part (ε'') of glass containing 15 mol% Li_2O at different frequencies

The temperature dependence of the real ε' and imaginary ε'' parts of dielectric constant at different frequencies for 55 P_2O_5 – 30 Na_2O –15 Li_2O glass are shown in Fig.12 and Fig.13 respectively. It is clear from Fig.12 that he obtained plots are straight and the values of ε' increase with increasing temperature and also with decreasing frequency which is normal in oxide glasses and this cannot be taken as indication for spontaneous polarization [A. A. Bahgat et al. (2001)].

A similar behavior is observed in Fig.13 for the variation of ε'' with temperature. This can be explained by means of dielectric polarization mechanism of the material. Among various polarization, deformational polarization (electronic and ionic) and relaxation polarization (dipolar and space charge polarization) that contribute to the dielectric constant. Electronic and ionic polarizations are active in high frequency range, while the other two mechanisms prevail in the low frequency range [S. Kurien et al. (2006), I. Bunget et al. (1984)]. The increase of both ε' and ε'' toward the low frequency region may be attributed to space charge polarization. As the frequency increases, the polarizability contribution from ionic source decreases and finally disappear [K. H. Mahmoud et al. (2011)].

Table.4 Shows the dependence of the real ε' and imaginary ε'' parts of dielectric constant at room temperature and frequency 3 MHz on concentration of Li_2O mol%.

Table.4 The variation of the real ε' and imaginary ε'' parts of dielectric constant at room temperature and frequency 3 MHz on concentration of Li_2O mol%

Composition of 55 P_2O_5 – (45-x) Na_2O – x Li_2O x (mol %)	Real part (ε') of dielectric constants (cm)	Imaginary part (ε'') of dielectric constants (cm)
3	4.42455	6.12816
10	5.92576	9.48849
15	11.55158	10.4
30	9.61353	10.2387
35	4.61211	8.55072

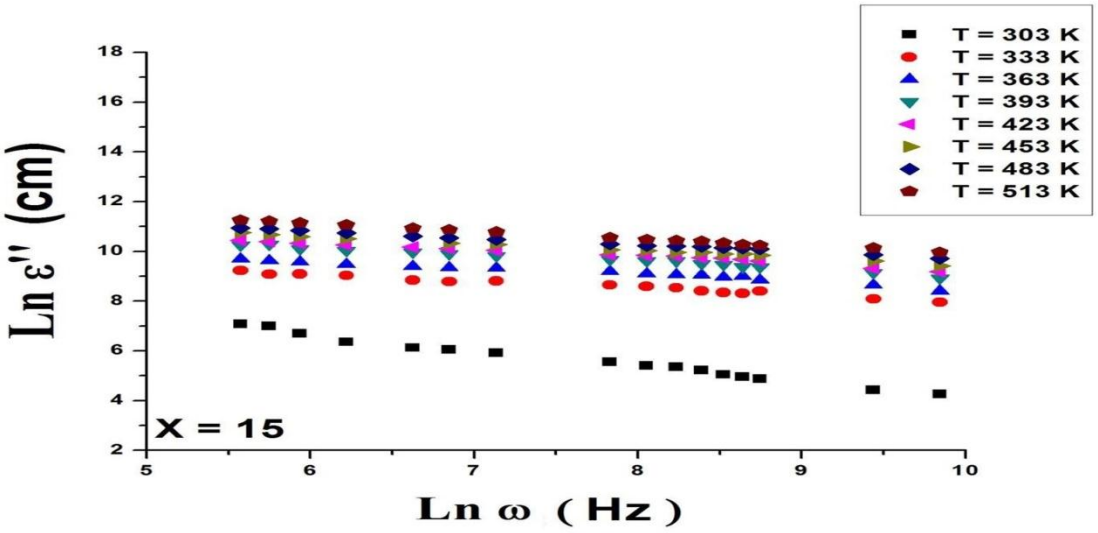

Fig.14. Frequency dependance of imaginary part (ε') of glass containing 15 mol% Li_2O at different temperatures

Fig.14 shows the variation of Ln ε'' with Ln ω for the investigated samples. It is clear from this figure that the obtained curves are straight lines at various temperatures. According to Guntini et al [J. C. Guntini et al. (1981)] ε'' at a particular frequency in the temperature range where dielectric dispersion occurs, is given by:

$$\varepsilon'' = B\,\omega^{m} \qquad (9)$$

The power m of this equation was calculated from the negative slopes of the obtained straight lines of Fig.14 at different temperatures.

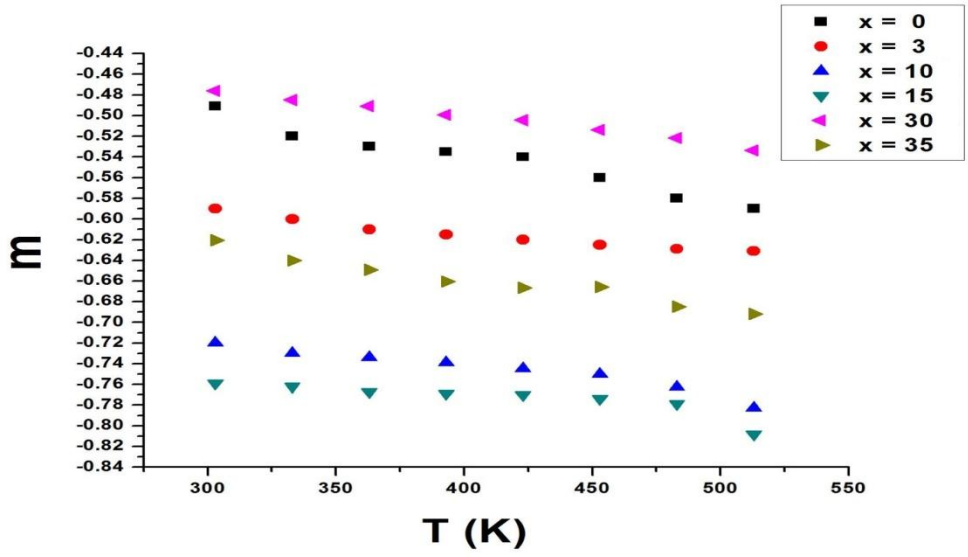

Fig.15. Temperature dependance of the investigated glasses for exponent m at different concentrations of Li_2O mol%

The variation of the obtained values of m with temperature for different concentration of Li_2O is shown in Fig.15. Fig.15 shows that m decreases with increasing temperature. According to Guintini et al the exponent m can be related to the temperature and the maximum barrier height W_m through the following equation:

$$m = -4K_BT/W_m \qquad (10)$$

Table.5 Shows the variation of the obtained values of the maximum barrier height Wm at different concentrations of Li_2O mol%

Composition of 55 P_2O_5 – (45-x) Na_2O – x Li_2O x (mol %)	Maximum barrier height (W_m) (eV)
0	0.61
3	0.68
10	0.71
15	0.59
30	0.702
35	0.728

4- Conclusion

Transparent glasses of 55 P_2O_5 - (45-x) Na_2O - xLi_2O ($0 \leq x \leq 35$) were prepared using the melt quenching technique. All prepared glasses are amorphous as confirmed by X-Ray diffraction. The increase of Li_2O concentration decreases the glass transition temperature (T_g) and decreases crystallization temperature (T_c) except for glass contains 15 mol% Li_2O which has the maximum value for T_g and T_c and this glass exhibits highest thermal stability. Density, molar volume and oxygen packing density insure that Li_2O incorporated in sodium phosphate glass by increasing Li_2O mol% concentration. The experimental and theoretical densities follow the similar trend. The dc and ac conductivity and their related conduction mechanisms of the investigated glasses were analyzed. Activation energies ΔE_{dc1} & ΔE_{ac1} and ΔE_{dc2} & ΔE_{ac2} at low and high temperatures are calculated. It was found the behavior of both ΔE_{dc} and ΔE_{ac} are the same.

The ac conductivity studies of investigated glasses have been carried out at different concentration of Li_2O mol% and the data has been analyzed by using Almond-West power law

$$\sigma_{ac} = \sigma(0) + A \cdot \omega^s \qquad (11)$$

The power law exponent S is found to decrease with increasing temperature and exhibits lower values in highly modified glasses. The correlated barrier hoping (CBH) seems to be the most interesting model related to the obtained results.

The dielectric parameters ε' and ε'' are found to increase with the increase in temperature and their variation with Li_2O mol% pass through a maximum at 15 mol% Li_2O (Table 2). These results would be discussed by means of dielectric polarization mechanism of material. The values of the maximum barrier height W_m obtained from Guitine equation were found to increase with increasing of the concentration of Li_2O mol% except 15 mol% Li_2O glass.

References

A. Ben Rasem, F. Hlel, K. Guidara, M. Gargouri, J. Alloys Compds. 385 **(2009)** 718.

A.A. Bahgat, Y.M. Abou eZeid, Phys. Chem. Glasses 42 **(2001)** 51.

A.Bhide, K.Hariharan, Mater.Chem.Phys. 105 **(2007)** 213.

A.V.Chandrasekhar, A.Radhapathy, B.I.Reddy, Opt.Mater. 22 **(2003)** 215.

A.Yamano, M.Morishita, G.Park, T.Sakamoro, H.Yamauchi, T.Nagakane, M.Ohji, A.Sakamoto, T.Sakai, J.Electrochem. Soc., 161 **(2014)** A1094-A1099.

D. P. Almond, C. C. Hunter, A. R. West, J. Mater. Sci. 19 **(1984)** 3236.

D.D.Ramteke, R.E.Kroon, H.C.Swart, J.Non-Cryst. Solids 457 **(2017)** 157-163.

G.E. Pike, Phys. Rev. B6 **(1972)** 157.

I. Bunget, M. Popescu, Phys. Solid Dielectric, Elsevier, New York, **1984**.

I.Abrahams, E.Hadzifejzovic, Solid State Ionic 134 **(2000)** 249.

J. C. Guntini, J. V. Zan Chetta, D. Julien, R. Eholie, P. Houenou, J. Non-Cryst. Solids 45 (**1981)**.

K. H. Mahmoud, F. M. Abdel-Rahim, K. Atef, Y. B. Saddeek, Current Applied Physics 11 **(2011)** 55-60.

Kirk-Othmar, Encyclopedia of Chemical Technology, Clarenden Press, Oxford**, 1963,** P.812.

L. Bih, L. Abbas, S. Mohdachi, A. Nadiri, J. Mol. Stract. 891 (**2008)** 173-177.

M. J. Miah, A. K. M. Akther Hossain, Acta Metall. Sin. (Engl. Lett.) **(2016).**

M.Altaf, M.A.Chaudhry, S.A.Siddiqi, Material Chemistry and Physics 71 **(2001)** 28-33.

Nehal Aboulfotoh, Yahia Elbashar, Mohamed Ibrahem, Mohamed ElOkr, Ceramics International 40 **(2014)** 10305-10399.

Paramjyot KomarJha, O.P.Pandey, K.Singh, J.Mol.Struct. 1094 (**2015)** 174-182.

Peipei Chen, Haitau Wu, Ya Qu and Yunlong Yue, Asian Journal of Chemistry Vol. 27, No.5 **(2015)** 1663-1666.

R.H. Chen, R.Y. Chang, C.S. Shem. Solid State Ion. 177 **(2006)** 2857.

R.K.Brow, J.Non-Cryst.Solids 263-264 **(2000)** 1.

R.K.Brow, J.Non-Cryst.Solids, 263-264 **(2000**) 1.

S. Kurien, J. Mathew, S. Sebastian, S.N. Pottv, Kc. George. Mater.Chem.Phys. 98 **(2006)** 470.

S. Rani, S. Sanghi, A. Agarwal, W. P. Seth, Spectrochim. Acta. Part., A74 **(2008)** 673-677.

S.R. Elliot, Philos. Mag. B.36 **(1978)** 129.

Samir Y.Marzouk, Materials Chemistry and Physics 114 **(2009)** 188-193.

Sh. A. Mansour, I. S. Yahia, G. B. Sakr, Solid State Communication 150 **(2010)** 1386 – 1391.

V.C.Veerana Gowda, R.V.Anavekar, Solid State Ionics 176 **(2005)** 1343-1401.

Yahia H.Elbashar, Ali M.Badr, Haron A.Elshaikh, Ahmed G.Mostafa, Ali M.Ibrahim, Processing and Application of Ceramics 10 (4) **(2016)** 277-286.

Yang Lia, Feng Song, Guozhi Jia, Yan bang, Yi Tang, Results in Physi**, (2017)** 1987-1992.

تحضير و توصيف زجاجيات فوسفات الصوديوم المعدلة بأُكسيد الليثوم

[a]محمد عصام سيد، [b]محمد محمود العقر، [c]ليلي أبراهيم سليمان، [d]حمدية عبد الحميد زايد

[a] مدرس مساعد-قسم الفيزياء-الاكاديمية الحديثة للهندسة و التكنولوجيا-المعادي-القاهرة-مصر
[b] أستاذ فيزياء الجوامد-قسم الفيزياء-كلية العلوم-جامعة الأزهر-القاهرة-مصر
[c] أستاذ فيزياء الجوامد-قسم الفيزياء-المركز القومي للبحوث-القاهرة-مصر
[d] أستاذ فيزياء الجوامد-قسم الفيزياء-كلية البنات-جامعة عين شمس-القاهرة-مصر

في هذا البحث تم تحضير زجاج شفاف من $55\ P_2O_5 - (45 - x)\ Na_2O - (x)\ Li_2O$ حيث ان $(x = 0, 3, 10, 15, 30, 35)$ بأستخدام تقنية الصهر و التبريد المفاجيء. و قد تم فحص العينات بأستخدام تقنية حيود أشعة أكس (XRD) و اثبتت النتائج ان جميع العينات ذات طبيعة أمورفيه. و قد تم تعيين كلاً من درجة التحول للزجاج (T_g) و درجة التبلر (T_c) بأستخدام تقنية (DTA) و قد أتضح من النتائج ان الزجاج الذي يحتوي علي 15 mol% Li_2O له أعلي درجة ثبات حراري. و كذلك تم قياس كلاً من الكثافة و الحجم المولاري للعينات المحضرة. و تم دراسة الخواص الكهربية لكل من التيار المستمر و التيار المتردد و معاملات ثابت العزل ε' و ε'' . و من الدراسة تم تعيين طاقتي التنشيط ΔE_{dc1} و ΔE_{dc2} عند درجات الحرارة المنخفضة و المرتفعة و كذلك ΔE_{ac1} و ΔE_{ac2} . و قد تم شرح ميكانيكية grain resistance عند 300K بأستخدام Cole-Cole plot. لتعيين ميكانيكية التوصيل و تم دراسة الموصلية الكهربية للتيار المتردد عند ترددات مختلفة و تم تحليلها علي اساس correlated barrier hopping (CBH) و قد وجد ان قيم exponent (s) تتراوح ما بين ٠.٦٢ – ٠.٩ و بناءً عليه يعتبر (CBH) هو انسب موديل متفق مع النتائج. و كذلك تم دراسة معاملات ثابت العزل ε' و ε'' و مدي تغييرها مع الترددات المختلفة و تركيزات Li_2O mol% و تم شرح النتائج بواسطة dielectric polarization mechanism of material. و كذلك تم حساب قيمة maximum barrier height (W_m) بأستخدام معادلات Guitini و وجد انه يزداد بزيادة Li_2O mol%.